microbiology research

MDPI

Article

Genome-Wide Identification of Cotton MicroRNAs Predicted for Targeting Cotton Leaf Curl Kokhran Virus-Lucknow

Muhammad Aleem Ashraf [1,2,*,†], Judith K. Brown [3,†], Muhammad Shahzad Iqbal [4] and Naitong Yu [1,*]

[1] Institute of Tropical Biosciences and Biotechnology, Chinese Academy of Tropical Agricultural Sciences, Haikou 571101, China
[2] Institute of Biological Sciences, Faculty of Natural and Applied Sciences, Khwaja Fareed University of Engineering and Information Technology, Rahim Yar Khan 64200, Pakistan
[3] School of Plant Sciences, The University of Arizona, Tucson, AZ 85721, USA; jbrown@ag.arizona.edu
[4] Department of Biochemistry, University of Okara, Okara 56300, Pakistan; shahzad.iqbal@uo.edu.pk
* Correspondence: ashraf.muhammad.aleem@gmail.com (M.A.A.); yunaitong@163.com (N.Y.)
† These authors contributed equally to this work.

Abstract: Cotton leaf curl Kokhran virus (CLCuKoV) (genus, *Begomovirus*; family, *Geminiviridae*) is one of several plant virus pathogens of cotton (*Gossypium hirsutum* L.) that cause cotton leaf curl disease in Pakistan. Begomoviruses are transmitted by the whitefly *Bemisia tabaci* cryptic species group and cause economic losses in cotton and other crops worldwide. The CLCuKoV strain, referred to as CLCuKoV-Bur, emerged in the vicinity of Burewala, Pakistan, and was the primary causal virus associated with the second CLCuD epidemic in Pakistan. The monopartite ssDNA genome of (2.7 Kb) contains six open reading frames that encode four predicted proteins. RNA interference (RNAi)-mediated antiviral immunity is a sequence-specific biological process in plants and animals that has evolved to combat virus infection. The objective of this study was to design cotton locus-derived microRNA (ghr-miRNA) molecules to target strains of CLCuKoV, with CLCuKoV-Lu, as a typical CLCuD-begomovirus genome, predicted by four algorithms, miRanda, RNA22, psRNATarget, and RNA hybrid. Mature ghr-miRNA sequences (n = 80) from upland cotton (2n = 4x = 52) were selected from miRBase and aligned with available CLCuKoV-Lu genome sequences. Among the 80 cotton locus-derived ghr-miRNAs analyzed, ghr-miR2950 was identified as the most optimal, effective ghr-miRNA for targeting the CLCuKoV-Lu genome (nucleotide 82 onward), respectively, based on stringent criteria. The miRNA targeting relies on the base pairing of miRNA–mRNA targets. Conservation and potential base pairing of binding sites with the ghr-miR2950 were validated by multiple sequence alignment with all available CLCuKoV sequences. A regulatory interaction network was constructed to evaluate potential miRNA–mRNA interactions with the predicted targets. The efficacy of miRNA targeting of CLCuKoV was evaluated in silico by RNAi-mediated mRNA cleavage. This predicted targets for the development of CLCuD-resistant cotton plants.

Keywords: computational algorithms; cotton leaf curl Kokhran virus; microRNA prediction; plant host–begomovirus interactions; RNA interference; target binding sites

Citation: Ashraf, M.A.; Brown, J.K.; Iqbal, M.S.; Yu, N. Genome-Wide Identification of Cotton MicroRNAs Predicted for Targeting Cotton Leaf Curl Kokhran Virus-Lucknow. *Microbiol. Res.* **2024**, *15*, 1–19. https://doi.org/10.3390/microbiolres15010001

Academic Editors: Ahmed M. Abdel-Azeem and Awatif Abid Al-Judaibi

Received: 27 September 2023
Revised: 12 December 2023
Accepted: 15 December 2023
Published: 19 December 2023

1. Introduction

The allotetraploid upland cotton (*Gossypium hirsutum* L.) is an economically important fiber-producing industrial cash crop grown on several continents and represents ~40% of agricultural outputs globally. Cotton is a prized natural textile fiber composed of 90% cellulose and a renewable natural fiber resource that supplies the global textile industry. Quality parameters of cotton fibers determine the economic value of the crop for the textile industry [1–3]. The allotetraploid upland cotton genome has 52 chromosomes (2n = 4x = 52) [4,5]. The first draft genome and physical map for upland allotetraploid cotton was released in 2015 [6].

Cotton leaf curl disease (CLCuD) causes major damage to the cotton crop in Pakistan and has been associated with more than four virus species, including CLCuKoV belonging to the genus *Begomovirus* (*Geminiviridae*) [7,8], a monopartite begomovirus and betasatellite complex [9–13]. Members of the genus are transmitted by the whitefly *Bemisia tabaci* cryptic species group, which is characterized by host range plasticity and variable efficiencies of begomovirus transmission [14–18].

Cotton leaf curl Kokhran virus-Lucknow (CLCuKoV-Lu) has recently emerged as a new 'strain' of CLCuKoV [19,20]. Begomoviruses have a circular, single-stranded (ss) DNA genome, with monopartite genomes encoding six proteins. Transcription and gene regulation are governed by sequences in the large intergenic region (LIR) and a bidirectional mode of transcription [12,21,22]. The plus (+) virion-sense (VS) and negative (−) complementary-sense (CS) strand encodes ORFs V1 and V2, and ORFs C1, C2, C3, and C4, respectively [15,19,23]. CLCuKoV-Lu was first reported in Lucknow in 2010 from guar (*Cyamopsis tetragonoloba*) plants exhibiting leaf curl symptoms [20]. Rolling circle amplification (RCA) is widely used to amplify and clone complete begomovirus genomes. Loop-mediated isothermal amplification (LAMP), quantitative real-time polymerase chain reaction (qPCR), multiplex PCR, and immunofluorescence assays are standard molecular diagnostics methods for detecting CLCuD-associated begomoviruses [24–30].

Despite ongoing efforts to manage CLCuD by controlling the whitefly vector, genetic resistance in cotton to multiple species and strains is required to manage this disease complex in Pakistan. The use of RNA interference (RNAi) has emerged as a robust tool for targeting microRNA-induced silencing complex (miRISC)-mediated gene silencing in eukaryotes [31–34]. RNAi is a double-stranded (ds) RNA-mediated, sequence-specific antiviral mechanism for inhibiting virus replication and transcription. The RNAi machinery consists of the core central components, Dicer and Argonaute. They are responsible for loading the 20–30 nucleotide RNA molecules, processing miRNA/miRNA* duplexes, and their incorporation into RISC. The dsRNA is cleaved into 21–24 nucleotides [35–39]. Plant microRNAs (miRNAs) are the smallest and most abundant highly conserved, non-coding, single-stranded (ss) RNA molecules, range in size from 18 to 24 nt in length, and are encoded by MIR genes. The endogenous miRNAs are important for regulating plant gene expression and key biological processes [40–42].

The molecular mechanisms that require mature miRNAs critical for normal growth in upland cotton have been studied [43–45]. Cotton-encoded miRNAs control biotic and abiotic stress response networks [46–50], whereas artificial miRNAs (amiRNA) are known to induce gene silencing that provides immunity against invading viruses [51]. An amiRNA has been constructed to induce gene silencing against a number of plant viruses [52], and the experimentally verified cotton plant locus-derived mature miRNAs have been shown to regulate gene expression. Finally, a subset of mature cotton miRNAs has been designed to predict target sites in genomes of the CLCuKoV species and strains with robust confidence [51].

The objective of this study was to identify genome-encoded miRNAs expressed by upland allotetraploid cotton that will target most or all CLCuKoV strains using an algorithmic in silico approach for miRNA predictions. To explore the mechanisms involved in host–virus interactions, miRNA–mRNA target site interactions were explored. Collectively, the results are expected to identify predicted ghr-miRNAs that can be used for the development of CLCuKoV-Lu-resistant cotton plants.

2. Materials and Methods

2.1. Biological Data

Eighty mature cotton locus-derived *G. hirsutum* microRNAs, or ghr-microRNAs (ghr-miR156-ghr-miR7514; accession no. MIMAT0005806-MIMAT0029164) (Table S1, Supplementary Materials) are available in the GenBank database. In another study, 78 stem-loop (precursor) cotton locus-derived ghr-miRNAs (ghr-MIR156-ghr-MIR7514) (accession IDs: MI0005638-MI0024206) have been published (Table S2). Cotton locus-derived ghr-miRNAs

were downloaded from miRBase v22.1 (http://mirbase.org/ accessed on 26 July 2019), which contains annotated miRNAs and associated biological information [53]. The complete genome of CLCuKoV-Lu, 2761 nucleotides in size (accession no. GU385879), was selected as the representative genome for miRNA screening. The sequence was downloaded from the NCBI GenBank database (http://ncbi.nlm.nih.gov, accessed on 19 December 2018) [54].

2.2. Target Prediction

Target predictions were based on an in silico approach that utilizes the most widely used, publicly available miRNA prediction algorithms, miRanda, RNA22, psRNATarget, and RNAhybrid. With these four algorithms, the 'most effective' miRNA binding sites of cotton miRNAs were predicted based on the CLCuKoV-Lu genome sequence (GU385879) (Table 1). Analysis was carried out for the *G. hirsutum* locus-derived ghr-miRNA sequences and CLCuKoV-Lu genome-predicted transcript sequences, inputted in FASTA format.

Table 1. Comparison of parameters among the miRNA–mRNA target prediction algorithms used in this study.

Tools	Algorithms	Seed Pairing	Multiple Target Sites	Translation Inhibition	Free Energy	Availability (Web/Code)
miRanda	Local alignment	+	+	+	+	+/+
RNA22	FASTA	−	+	−	+	+/−
psRNATarget	Smith–Waterman	−	+	+	−	+/−
RNAhybrid	Intermolecular hybridization	+	+	+	+	+/−
Tapirhybrid	FASTA	+	+	−	+	+/+
TargetSpy	FASTA	−	+	−	+	−/+
Targetfinder	FASTA	+	−	−	+	−/+

2.3. miRanda Algorithm

The miRanda algorithm offers seed-matching, scoring scheme, dynamic programming, and conservation consisting of three major steps to identify target sites since its release in 2003 [55], facilitates the prediction of candidate target sites (CTSs) based on minimum free energy, specifically taking into account RNA duplex dimerization and complementarity score of the target sequence [56]. The miRanda software was downloaded using the online source website (http://www.microrna.org/, accessed on 23 March 2019). Prediction analysis was carried out using the default parameters, with an MFE threshold of −20 Kcal/mol, score threshold of 140.00, gap open penalty of −9.000, gap extend penalty of −4.000, and scaling parameter of 4.00.

2.4. RNA22 Algorithm

The RNA22 algorithm implements a pattern-recognition approach for predicting target binding sites [57]. The RNA22 non-seed-based algorithm can be accessed on a web server (http://cm.jefferson.edu/rna22v1.0/, accessed on 26 January 2019). Biologically significant miRNA–mRNA interactions were predicted based on target patterns and maximum folding energy (MFE) [58] to identify optimal site complementarity, a unique feature of the RNA22 algorithm. The default parameters were used for the analysis of cotton miRNAs and the CLCuKoV-Lu genome sequence as templates, respectively, at 63% for x, 61% specificity, and an MFE of −15.00 Kcal/mol.

2.5. psRNATarget Algorithm

The psRNATarget algorithm is used to predict small RNA targets with plant-specific features, together with a seed-matching and -scoring scheme. Using the online website,

predicted binding sites of plant miRNAs are identified based on complementary scoring [59] while also reporting inhibition patterns [60]. The fasta sequence of the CLCuKoV-Lu genome was inputted with selected *G. hirsutum* miRNAs into the webserver (http://plantgrn.noble.org/psRNATarget, accessed on 26 October 2020). Target sites of cotton miRNAs were identified using the default criteria consisting of an expected cut-off of 6.5 and 'cleavage' as the mode of inhibition.

2.6. RNAhybrid Algorithm

The RNAhybrid algorithm is a seed-based, flexible online computational method that is based on intermolecular hybridization predictions of miRNA binding sites in the target sequence, using the MFE model set at −20.00 Kcal/mol, with site complementarity and seed match features [61]. The fasta sequence of CLCuKoV-Lu genome and miRNAs were uploaded to the webserver (http://bibiserv.techfak.uni-bielefeld.de/rnahybrid, accessed on 19 December 2020) for the analysis.

2.7. RNAfold and RNAcofold Algorithm

The RNAfold algorithm identifies accurate secondary structures associated with a target single-stranded (ss) miRNA precursor [62], which were uploaded to the web server (http://rna.tbi.univie.ac.at/cgi-bin/RNAWebSuite/RNAfold.cgi, accessed on 6 September 2022) for analysis. The RNAcofold algorithm estimates the co-folding free energy (ΔG) of RNA duplex sequences. The MFE and base pairing of miRNA–mRNA target duplex were predicted based on miRNA–mRNA interactions [63]. Also, FASTA sequences for each unique duplex pair were uploaded and analyzed with RNAcofold with default settings (http://rna.tbi.univie.ac.at/cgi-bin/RNAWebSuite/RNAcofold.cgi, accessed on 6 May 2022).

2.8. Mapping Network Interactions between miRNA and Virus Target Sequences

A Circos plot was produced using the CIRCOS algorithm and circos package v0.69-9R-Language [64].

2.9. Identification of miRNA Binding Sites

The predicted transcripts available for CLCuKoV strains were downloaded from the NCBI GenBank database (accessed on 26 March 2018), as follows: GU385879.2, AM421522.1, AJ496286.1, HF549182.1, and FN5520001.1 [19]. The MEGA X software v10.0.5 was used to align the conservation of binding affinity of predicted consensus miRNAs [65]. The MUSCLE algorithm was used to align the selected CLCuKoV genome sequences [66], and the miRNA binding site sequences were mapped using the CLUSTALW algorithm [67].

2.10. Statistical Analysis

The miRNA target predictions were analyzed and processed, and graphical representations were produced in R (version 3.1.1, software version 3.5.1) [68].

2.11. Virus Genome Annotation

The pDRAW32 DNA analysis (AcaClone 1.1.147) was used to annotate the ssDNA genome of CLCuKoV-Lu. The genome graphical output of the genome sequence characterization was carried out to identify coding and non-coding regions.

3. Results

3.1. Cotton-Encoded miRNAs–mRNA Interactive Pairs for the CLCuKoV-Lu Genome

The genome map of CLCuKoV-Lu, a circular ssDNA virus 2750 nucleotides in size was drawn based on predicted start and stop sites of virus open reading frame (ORFs) and non-coding sequences, respectively (Figure 1).

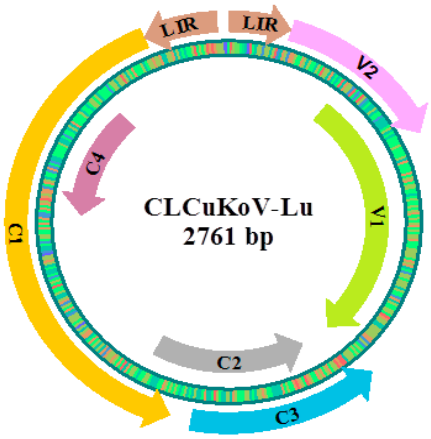

Figure 1. The CLCuKoV-Lu encodes six open reading frames (ORFs) indicated by the colored arrows. The plus (+) or virion-sense strand encodes ORFs (V1 and V2). The negative (−) strand encodes the complementary-sense strand ORFs, C1, C2, C3, and C4. Replication of the viral genome and transcription of the coding regions are under the control of the non-coding large intergenic region (LIR).

The CLCuKoV-Lu genome has six overlapping ORFs that encode viral proteins. Using the miRBase web-based tool for miRNA genomics and three distinct prediction algorithms (miRanda, RNA22, and psRNATarget), the cotton genome-encoded miRNAs possess the capacity to target the representative species genome, CLCuKoV-Lu. The CLCuKoV-Lu genome and experimentally verified mature cotton locus-derived ghr-miRNAs were downloaded from miRBase version 22 and evaluated for binding strength of miRNA–mRNA target interactions.

The CLCuKoV-Lu genome sequence was analyzed by searching for cotton miRNAs using the miRanda algorithm that predicted 11 miRNA–mRNA target pairs. The RNA22 predicted effective target binding sites in 11 cotton miRNAs affiliated with 11 loci in the CLCuKoV-Lu genome. The psRNATarget predicted 20 cotton miRNAs at 26 loci as cleavable target candidates, whereas the RNAhybrid approach predicted 76 miRNA–mRNA target pairs (Figure 2, Tables S3 and S4, and File S1).

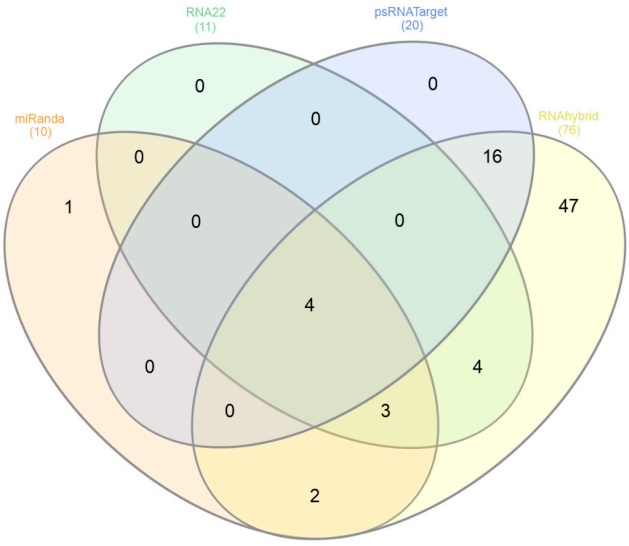

Figure 2. Venn diagram showing miRNA–mRNA target pairs in the CLCuKoV-Lu genome. Four widely used computational algorithms, miRanda, RNA22, psRNATarget, and RNAhybrid, were used to estimate host–virus interaction pairs. Binding sites were used to determine the degree of overlap predicted by the in silico algorithms consulted. The intersection map of the four computational tools reveals four commonly occurring ghr-miRNAs.

3.2. Viral V1-Encoding Coat Protein (CP)

The begomoviral V1 ORF 291–1061 (770 nt) encodes the coat protein (CP), which is required for encapsidation of the begomoviral ssDNA genome into virions, whitefly vector-mediated transmission, and virus movement [69–71]. The V1 was targeted by four predicted cotton locus-derived ghr-miRNAs: ghr-miR7486 (a, b) (locus 846), ghr-miR7497 (locus 349), and ghr-miR7506 (locus 509), based on the miRanda algorithm (Figure 3A). The RNA22 algorithm identified two miRNAs: ghr-miR169a (locus 691) and ghr-miR7512 (locus 917) (Figure 3B). The psRNATarget algorithm predicted 10 miRNAs: ghr-miR827 (a, b, and c) (locus 740), ghr-miR3476-5p (locus 765), ghr-miR7492 (a, b, and c) (locus 901), ghr-miR7497 (locus 459), ghr-miR7500 (locus 674), and ghr-miR7510a (locus 805) (Figure 3C). The RNAhybrid algorithm identified nine ghr-miRNAs: ghr-miR393, ghr-miR482 (a, b), ghr-miR7486 (a, b), ghr-miR7490, ghr-miR7504a, ghr-miR7510a, and ghr-miR7512 at nucleotide coordinates 611, 581, 849, 670, 694, and 917, respectively (Figure 3D, Tables 2, S3 and S4, and File S1).

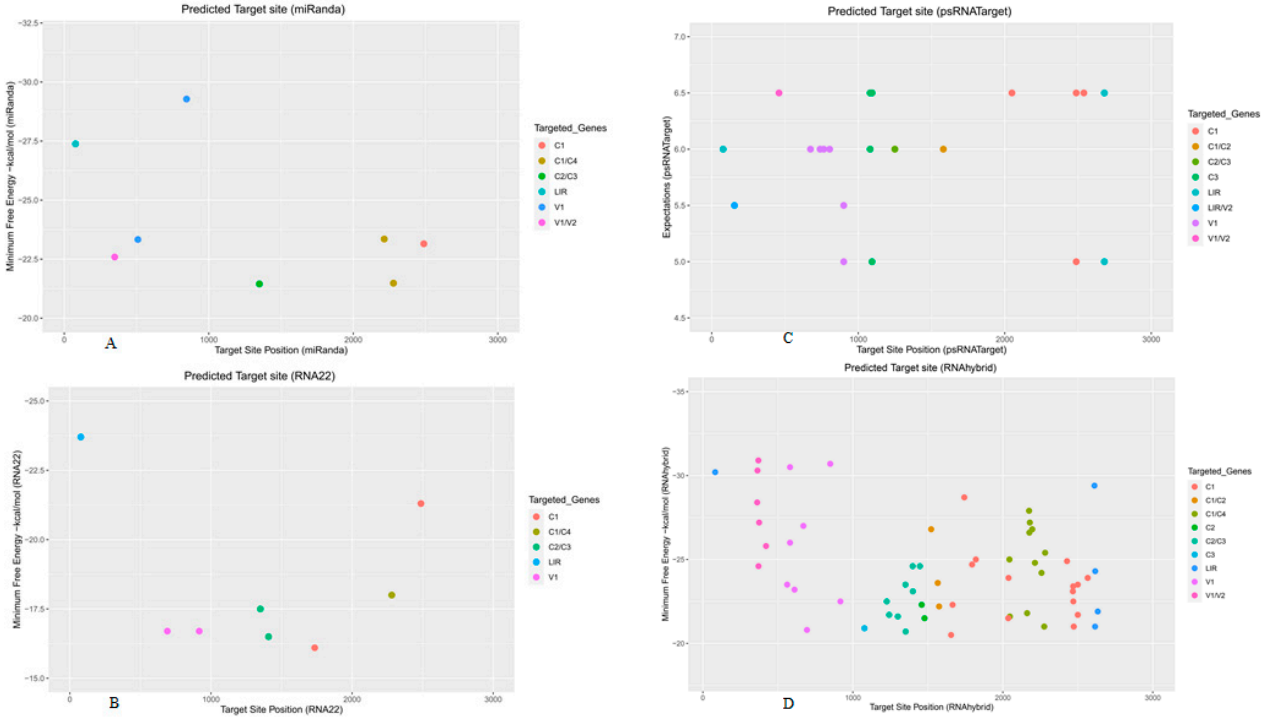

Figure 3. Predicted target sites of cotton ghr-miRNAs based on four widely used in silico miRNA–mRNA targets. (**A**) Prediction of miRNA binding sites based on the miRanda algorithm. (**B**) The miRNA target sites predicted by RNA22. (**C**) The psRNATarget predicted target sites. (**D**) The miRNA binding sites predicted by RNAhybrid. The miRNA target sites are indicated by colored dots.

3.3. Viral V2-Encoding Pre-Coat Protein

The begomovirus V2 ORF (131–487 nt) is 356 nucleotides in size and encodes the pre-coat protein. The V2 protein is involved in symptom development, movement, vector transmission, and regulation of gene expression [71–74]. The r-miR7497 was predicted to optimally target V2 at nucleotide 349 and 155 and 459, based on the miRanda and psRNATarget algorithms, respectively (Figure 3A,C). The RNAhybrid algorithm identified six ghr-miRNAs to target the overlapping region of V1 and V2 ORF: ghr-miR164, ghr-miR479, ghr-miR3476-5p, ghr-miR7497, ghr-miR7498, and ghr-miR7507 at nucleotide positions 375, 371, 421, 362, 370, and 364, respectively (Figure 3D; Tables 2, S3 and S4; File S1).

Table 2. Cotton ghr-miRNAs predicted to target the CLCuKoV ORF genome sequences.

CLCuKoV-Lu Gene	miRanda	RNA22	psRNATarget	RNAhybrid
V1	ghr-miR7486 (a, b), ghr-miR7506	ghr-miR169a, ghr-miR7512	ghr-miR827 (a, b, c), ghr-miR3476-5p ghr-miR7492 (a, b, c), ghr-miR7500 ghr-miR7510a	ghr-miR393, ghr-miR482 (a, b), ghr-miR7486 (a, b), ghr-miR7490, ghr-miR7504a, ghr-miR7510a, ghr-miR7512
V1/V2	ghr-miR7497		ghr-miR7497	ghr-miR164, ghr-miR479, ghr-miR3476-5p, ghr-miR7497, ghr-miR7498, ghr-miR7507
C1	ghr-miR7486 (a, b)	ghr-miR398, ghr-miR7486 (a, b)	ghr-miR7486 (a, b)	ghr-miR156 (a, b, c, d), ghr-miR162a, ghr-miR166b, ghr-miR169a, ghr-miR398, ghr-miR827 (a, b, c), ghr-miR2949-3p, ghr-miR3476-3p, ghr-miR7491, ghr-miR7492 (a, b, c), ghr-miR7500, ghr-miR7501, ghr-miR7505, ghr-miR7506
C2				ghr-miR394 (a, b), ghr-miR7504b
C1/C2			ghr-miR7510b	ghr-miR7485, ghr-miR7487, ghr-miR7514
C3			ghr-miR7484 (a, b), ghr-miR7492 (a, b, c)	ghr-miR7484 (a, b)
C2/C3	ghr-miR7513	ghr-miR7489, ghr-miR7513	ghr-miR396 (a, b)	ghr-miR167 (a, b), ghr-miR396 (a, b), ghr-miR2949(a-5p, b, c), ghr-miR7489, ghr-miR7493, ghr-miR7494, ghr-miR7511, ghr-miR7513
C4/C1	ghr-miR390 (a, b, c), ghr-miR7503	ghr-miR390 (a, b, c)		ghr-miR160, ghr-miR172, ghr-miR390 (a, b, c), ghr-miR399d ghr-miR7488, ghr-miR7495 (a, b), ghr-miR7503, ghr-miR7508, ghr-miR7509, ghr-miR7510b
LIR	ghr-miR2950	ghr-miR2950	ghr-miR2950	ghr-miR399 (a, b, c, e), ghr-miR2948-5p, ghr-miR2950,

3.4. Viral C1-Encoding Replication-Associated Protein

The C1 ORF (1505–2581), consisting of 1076 bases, encodes a replication-associated protein (Rep) that is essential for ssDNA replication and transcription [19,75–77]. miRanda predicted six miRNAs: ghr-miR390 (a, b, and c) (locus 2278), ghr-miR7486 (a, b) (locus 2488), and ghr-miR7503 (locus 2214) (Figure 3A). The C1 ORF gene was also targeted by six predicted miRNAs: ghr-miR390 (a, b, and c) (locus 2281), ghr-miR393 (locus 1735), and ghr-miR7486 (a, b) (locus 2488) by RNA22 (Figure 3B). Five potential miRNA candidates were predicted to silence the C1 gene by psRNATarget: ghr-miR7486 (a, b) (locus 2488), ghr-miR7505 (locus 2049), ghr-miR7510b (locus 1581), and ghr-miR7513 (locus 2540) (Figure 3C). The RNAhybrid algorithm predicted 21 ghr-miRNAs: ghr-miR156 (a, b, c, d), ghr-miR162a, ghr-miR166b, ghr-miR169a, ghr-miR398, ghr-miR827 (a, b, c), ghr-miR2949-3p, ghr-miR3476-3p, ghr-miR7491, ghr-miR7492 (a, b, c), ghr-miR7500, ghr-miR7501, ghr-miR7505, and ghr-miR7506 at nucleotide positions 2500, 1665, 2038, 1820, 2469, 2473, 1655, 2470, 1743, 2566, 2467, 2428, 2036, and 1795, respectively (Figure 3D, Tables 2, S3 and S4, and File S1).

3.5. Viral C2-Encoding Transcription Activator Protein

The C2 ORF of begomoviruses (1153–1599; 446 nt) encodes the transcriptional activator protein (TrAP) essential for symptom development in the plant host [15,78–80]. Among the CLCuKoV-Lu genes targeted, C2 had very few binding sites; nonetheless, several were identified as cotton miRNAs. The miRanda algorithm predicted the hybridization of ghr-miR7513 at locus 1350 in the overlapping region of C2 and C3 ORFs (Figure 3A). RNA22 predicted two miRNAs: ghr-miR7489 (locus 1408) and ghr-miR7513 (2540) in the C2 and C3 ORFs (Figure 3B). Three miRNA had predicted binding affinity with C2 with

respect to the psRNATarget: ghr-miR396 (a, b) at locus 1250 in the C2 and C3 overlapping ORFs and ghr-miR7510b at locus 1581 in the C2 and C1 overlapping ORFs (Figure 3C). RNAhybrid predicted cotton ghr-miRNAs: ghr-miR394 (a, b), ghr-miR7504b in the C2 ORF (Figure 3D, Tables 2, S3 and S4, and File S1).

3.6. Viral C3-Encoding Replication Enhancer Protein

The C3 ORF of begomoviruses (1058–1459) (401 nt) encodes a replication enhancer protein (REn) [81,82]. The psRNATarget algorithm identified five predicted miRNAs in ORF C3: (locus 1250), ghr-miR7484 (a, b) (1081), and ghr-miR7492 (a, b, and c) (1094). In addition, psRNATarget predicted in the overlapping region of C2 and C3: ghr-miR396 (a, b) (Figure 3C). The RNAhybrid algorithm predicted two cotton miRNAs targeting C3 ORF: ghr-miR7484 (a, b) at nucleotide position 1077. The RNAhybrid algorithm identified cotton miRNAs in the C2 and C3 overlapping region: ghr-miR167 (a, b), ghr-miR396 (a, b), ghr-miR2949 (a-5p, b, c), ghr-miR7489, ghr-miR7493, ghr-miR7494, ghr-miR7511, and ghr-miR7513 at genomic positions 1400, 1226, 1242, 1447, 1352, 1399, and 1350, respectively (Figure 4D, Tables 2, S3 and S4, and File S1).

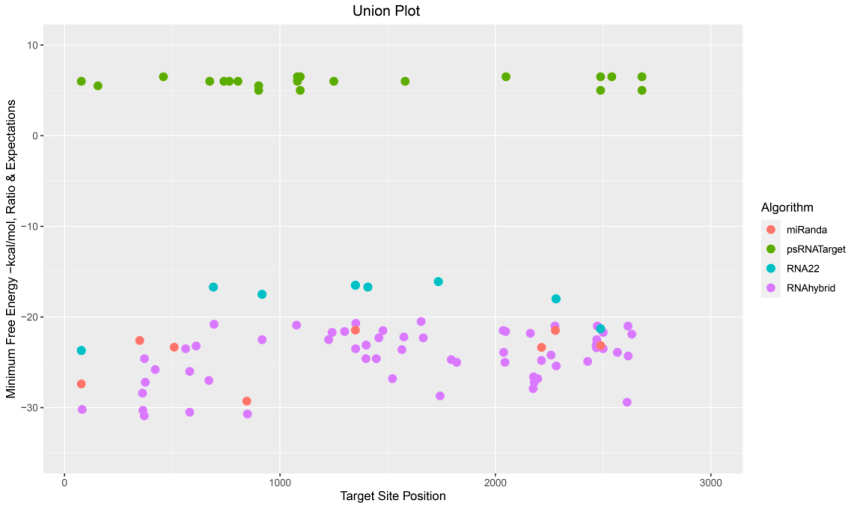

Figure 4. Union plot of prediction indicating the predicted miRNA target sites based on analysis of all algorithms used for evaluation of miRNA target sites, which are represented by colored dots.

3.7. Viral C4-Encoding Transcription Regulator Protein

The C4 ORF (2091–2429) of 338 bases in size encodes a transcription regulator protein that functions as a viral effector [77,83,84].

The miRanda and RNA22 algorithms both predicted the binding of ghr-miR390 (a, b, and c) at consensus genomic locus 2281. The ghr-miR7503 targeting the C1 gene showed binding affinity at nucleotide 2214 (Figure 3A,B). The RNAhybrid algorithm predicted cotton miRNAs in the C4-C1 overlapping region: ghr-miR160, ghr-miR172, ghr-miR390 (a, b, and c), ghr-miR399d, ghr-miR7488, ghr-miR7495 (a, b), ghr-miR7503, ghr-miR7508, ghr-miR7509, and ghr-miR7510b at nucleotide positions 2044, 2177, 2196, 2047, 2258, 2276, 2214, 2282, 2162, and 2175, respectively (Figure 3D, Tables 2, S3 and S4, and File S1).

3.8. Large Intergenic Region of Cotton Leaf Curl Begomoviruses

The large intergenic region (LIR) drives transcriptional regulation of begomovirus V1 and C1 ORFs [21,22,85]. Four algorithms (miRanda, RNA22, psRNATarget, and RNAhybrid) predicted a hybridization binding site of ghr-miR2950 at consensus genomic locus 82 of CLCuKoV that would target the LIR (Figure 3A–D). In addition, the LIR was predicted to be targeted by three miRNAs, ghr-miR7484 (a, b) and ghr-miR7497, as shown for the psRNATarget (Figure 3C). The RNAhybrid predicted cotton ghr-miRNAs in LIR:

ghr-miR399 (a, b, c), ghr-miR2948-5p, and ghr-miR2950 at nucleotides 2633, 2616, 2611, and 82, respectively (Figure 3D; Tables 2, S3 and S4, and File S1).

3.9. Prediction of Universal Cotton Plant-Encoded miRNAs

The target miRNAs predicted to silence expression of CLCuKoV-Lu genes were the miRNAs ghr-miR2950, ghr-miR7486 (a, b), and ghr-miR7513, based on analysis with all four algorithms considered in this study (Figures 2–4; Table S3 and File S1).

3.10. Prediction of Cotton Plant Genome miRNAs

Of the 80 targeting mature *G. hirsutum* locus-derived ghr-miRNAs investigated, 7 *G. hirsutum* ghr-miRNAs: ghr-miR390 (a, b, c), ghr-miR7484 (a, b), ghr-miR7503, and ghr-miR7512 at nucleotide positions 2281, 1081, 2214, and 917, respectively, were predicted as potential binding sites in the CLCuKoV-Lu genome consensus, detected by at least prediction tools (Tables 2–4). Of 80 cotton miRNAs, three conserved *G. hirsutum* ghr-miRNAs were identified.

Table 3. Target binding sites of predicted consensus cotton ghr-miRNAs identified in the CLCuKoV-Lu genome.

Cotton miRNA	Target Site miRanda	Target Site RNA22	Target Site psRNATarget	Target Site RNAhybrid	MFE *miRanda	MFE ** RNA22	Expectation psRNATarget	MFE *RNAhybrid
ghr-miR390 (a, b, c)	2278	2281			−21.48	−18.00		
ghr–miR2950	78	78	78	82	−27.38	−23.70	6.5	−30.20
ghr–miR7484 (a, b)			1081	1077			6.5	−20.90
ghr-miR7486 (a, b)	2488/846	2488	2488	849	−23.15/−29.28	−21.48	5.0	−30.70
ghr-miR7503	2214			2214	−23.35			−27.00
ghr-miR7512		917		917		−16.70		−23.50
ghr-miR7513	1350	1350		1351	−21.45	−17.50		−26.80

* MFE represents minimum free energy while MFE ** is the abbreviation of the maximum folding energy.

Table 4. Binding sites of predicted consensus cotton ghr-miRNAs targets.

miRNA ID	Accession ID	Mature Sequence (5′–3′)	Target Genes ORF(s)	Target Binding Locus Position
ghr-miR390a	MIMAT0005815	AAGCUCAGGAGGGAUAGCGCC	C1/C4	2278–2298
ghr-miR390b	MIMAT0005816	AAGCUCAGGAGGGAUAGCGCC	C1/C4	2278–2298
ghr-miR390c	MIMAT0005817	AAGCUCAGGAGGGAUAGCGCC	C1/C4	2278–2298
ghr-miR2950	MIMAT0014348	UGGUGUGCAGGGGGUGGAAUA	LIR	78–97
ghr-miR7484a	MIMAT0029124	UUUGUAUAUUAGAUCAAAGAGCAA	C3	1081–1105
ghr-miR7484b	MIMAT0029125	UUUGUAUAUUAGAUCAAAGAGCAA	C3	1081–1105
ghr-miR7486a	MIMAT0029127	AAGGAAGCGCUUUGUCCACGUGGA	C1/V1	2488–2510/846–871
ghr-miR7486b	MIMAT0029128	AAGGAAGCGCUUUGUCCACGUGGA	C1/V1	2488–2510/871
ghr-miR7503	MIMAT0029150	AGAUCGAUGGCUGAACAAGUUAGA	C4/C1	2214–2237
ghr-miR7512	MIMAT0029161	UGCUACUUGUAGUUAUGCAUG	V1	917–938
ghr-miR7513	MIMAT0029162	AAUCAGCCAGGAAUCGUUUGA	C2/C3	1350–1372

The ghr-miR7486 (a, b) and ghr-miR7513 were identified as predicted consensus genomic binding sites at nucleotide positions 2488 and 1350, respectively, based on the consensus of multiple algorithms used herein. Here, only one *G. hirsutum* ghr-miRNA (ghr-miR2950) was predicted to have a target binding site at common genomic position 82 when analyzed by all of the algorithms tested (Tables 2–4, Figure 5). For the CLCuKoV-Lu genome, ghr-miR2950 was predicted to target the non-coding LIR, while ghr-miR2488 (a, b) targeted the coding region C1 gene, and ghr-miR7513 targets the overlapping region of ORFs C2/C3 (Figure 5 and Table 3).

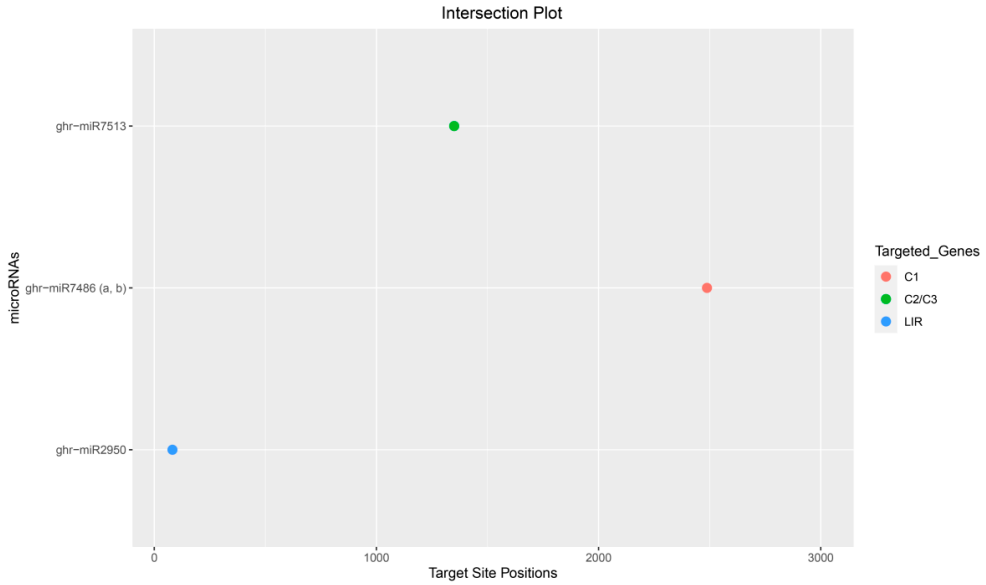

Figure 5. Intersection plot of predicted consensus binding sites of cotton ghr-miRNAs predicted by multiple algorithms with predicted binding sites confirmed by at least three algorithms in the consensus reference genome for the CLCuKoV-Lu species.

Of the 11 predicted consensus *G. hirsutum* ghr-miRNAs, only 1 ghr-miRNA of *G. hirsutum* (ghr-miR2950 at nucleotide position 78–97), with an MFE of −27.38 Kcal/mol, was detected as top effective candidate (Tables 4 and 5). The 'cleavage' efficacy of the ghr-miR2950 was verified against CLCuKoV-Lu by RNAi-mediated suppression, as concluded by Brodersen [86].

Table 5. Features of predicted consensus cotton *G. hirsutum* ghr-miRNA target pairs.

Cotton miRNA	miRNA Target Pair	Locus Position	MFE (Kcal/mol)	Score	Complementarity (%)	Mode of Inhibition
ghr-miR2950	Query: 3′ auaag-GUGGGGGACGUGUGGu 5′ | : | : | | | | | | | | | : Ref: 5′ aataaCGCTCCC-GCACACTa 3′	78–97	−27.38	142	93.33	Cleavage
ghr-miR7486 (a, b)	Query: 3′ aggUGCACCUGUU-UCGCGAAGGAa 5′ | : | | | : | | | | : | | | | | | | Ref: 5′ tgaATTTGGG-AAAGTGCTTCCTc 3′	2488–2510	−23.15	171	90.00	Cleavage
ghr-miR7513	Query: 3′ agUUUGCUAA--GGACCGACUAa 5′ : : | | | : | | | | | | | | | | | Ref: 5′ atGGACGGTTGACGTG-GCTGATg 3′	1350–1372	−21.45	162	85.00	Cleavage

3.10.1. Visualization of miRNA Targets

To validate the predicted miRNA–mRNA target–gene interaction analysis, a Circos plot was constructed to identify host miRNA targets. The mature cotton locus-derived ghr-miRNAs are indicated on the CLCuKoV-Lu genome sequence maps (Figure 6).

3.10.2. Secondary Structure Analysis

The efficacy of the predicted consensus miRNAs was analyzed based on secondary structure. Secondary structures were predicted based on manually curated cotton precursors. The MFE was used as the standard criterion for analyzing the stability of the

CLCuKoV-Lu RNA structure. The diagrams show the characteristic features of seven consensus precursors (Table 6).

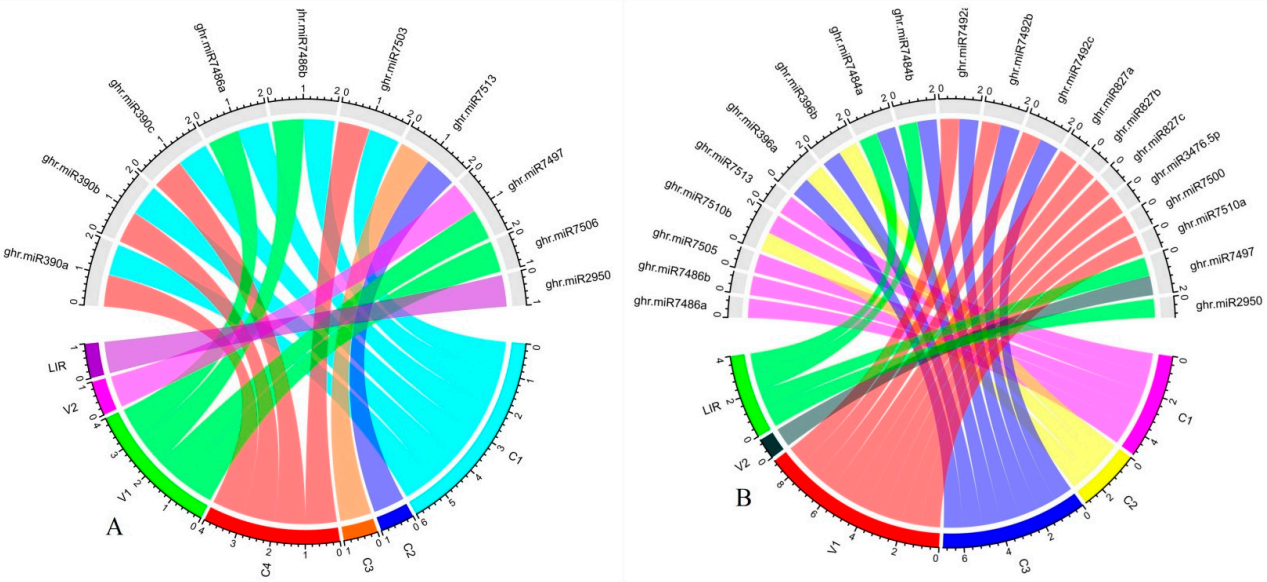

Figure 6. A Circos plot showing cotton locus-derived ghr-miRNAs targeting CLCuKoV-Lu ORFs. CLCuKoV-Lu ORFs are represented with colored lines. (**A**) Interaction Circos map for the seed-based algorithm miRanda. (**B**) Interaction Circos map for the non-seed-based psRNATarget algorithm.

Table 6. Features of the precursor of the predicted cotton locus-derived ghr-miRNAs.

miRNA ID	Accession ID	Length Precursor	MFE */Kcal/mol	AMFE **	MFEI ***	(G + C)%
ghr-MIR2950	MI0013555	108 nt	−48.10	−44.53	−1.002	44.44
ghr-MIR7486a	MI0024169	105 nt	−81.90	−78.00	−1.436	54.29
ghr-MIR7486b	MI0024170	101 nt	−69.50	−68.81	−1.336	51.49
ghr-MIR7513	MI0024204	103 nt	−36.70	−35.63	−0.965	36.89

* MFE is minimum free energy. ** AMFE is the abbreviation of adjusted free energy. *** MFEI is defined as free energy index.

3.10.3. Free Energy (ΔG) Computational Analysis

To validate the predicted miRNAs, the free energy (ΔG) of the duplexes was analyzed by computing the free energy (ΔG) of four consensus cotton locus-derived ghr-miRNAs (Table 7).

Table 7. Free energy (ΔG) estimates of the consensus cotton ghr-miRNA–mRNA.

miRNA ID	miRNA–mRNA Sequence (5′–3′)	ΔG Duplex (Kcal/mol)	ΔG Binding (Kcal/mol)
ghr-miR2950	5′ UGGUGUGCAGGGGGUGGAAUA 3′ 5′ AATAACGCTCCCGCACACTA 3′	−24.80	−24.37
ghr-miR7486 (a, b)	5′ AAGGAAGCGCUUUGUCCACGUGGA 3′ 5′ TGAATTTGGGAAAGTGCTTCCTC3′	−22.70	−17.41
ghr-miR7513	5′AAUCAGCCAGGAAUCGUUUGA 3′ 5′ ATGGACGGTTGACGTGGCTGATG 3′	−20.90	−17.74

3.10.4. Conserved Begomoviral Genome Binding Sites

Among the predicted genome binding sites, the greatest conservation among the different CLCuKoV-Lu strains was found for ghr-miR2950 (78–97) (Figure 7).

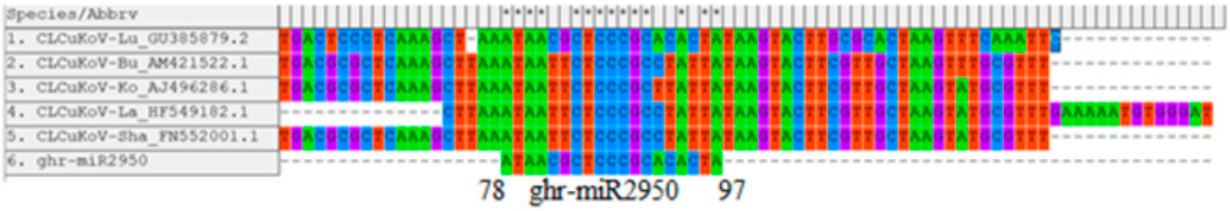

Figure 7. Multiple sequence alignment of the conserved bases indicating the sites in the genome of CLCuKoV that were targeted by ghr-miR2950.

4. Discussion

The CLCuD disease is caused by a complex of species and strains endemic to Pakistan. The results of this study have identified, based on several well-known computational approaches and validated with different algorithms, three cotton miRNAs in 80 mature miRNAs with the potential to target the genome of CLCuKoV-Lu and other CLCuKoV strains. For several decades, the leaf curl disease caused by CLCuKoV and related begomovirus strains and species has limited cotton production in Pakistan [9,11,12,87,88]. By exploiting adaptive host defenses that can be mounted against CLCuKoV using cotton miRNAs, disease management may become a reality. The false-positive predictions were filtered using the computational algorithms described above to evaluate predicted miRNAs at three different levels. The performance of data-driven algorithms was validated at the 'union of intersections' level in relation to predicted biological data, and the potential cotton miRNA–mRNA target interactions were validated (Figure 5).

The results of this study predict mature cotton genome-encoded miRNAs (ghr-miR2950, ghr-miR7486 (a, b)) that are expected to target CLCuKoV-Lu (and other CLCuKoV strains) toward developing leaf curl resistance in cotton. The miRNAs identified in this study are predicted to interact with the C1 and LIR of CLCuKoV-Lu. These results indicate that an evolutionarily conserved cotton miRNA, ghr-miR2950, has been selectively employed by CLCuKoV-Lu to overcome host defenses and cause leaf curl disease in cotton. Previous studies have reported host–virus interactions using online computational tools to identify the binding affinity of genome-encoded miRNAs in RTV1 [89], SCBV [90], SCYLV [91], ZYMV [92], SCBGAV [93], ToBRFV and PhCMoV [94], RYMV [95], MCMV [96], and ICMV-Ker [97]. Here, similar results were obtained for a predominant causal begomovirus of the cotton leaf curl disease using online computational tools previously shown to facilitate optimal target predictions for sugarcane- and rubber tree-infecting plant viruses [89–91,93].

In this study, multiple in silico algorithms were used to enable computational predictions, i.e., consensus target binding sites of ghr-miR2950 at a locus (locus 78), ghr-miR7484 (a, b) locus (1081) and ghr-miR7486 (a, b), and locus (2488), whereas no binding site was predicted by TAPIR. Host plant-delivered plant miRNAs can induce the degradation of viral targets through base pairing. The results demonstrate that CLCuKoV-Lu genomic components (C1 and LIR) are expected to be highly susceptible to targeting by consensus miRNAs identified here. Among the 80 cotton miRNAs identified, the ghr-miR2950 was shown to harbor a consensus genomic binding site occurring within the large intergenic region (LIR) of the CLCuKoV-Lu genome (Figure 7). The LIR governs the bidirectional mode of transcription of C1 and V1 genes and functions as a bidirectional promoter [21,22]. The use of the union and intersection prediction approaches was essential for controlling false-positive prediction. Union-level prediction relies on a combination of target prediction algorithms to find 'true targets'. In this study, the sensitivity level of data predictions was increased at the cost of lower-level specificity. In contrast, the intersectional approach combines two or more algorithmic tools, and a specific threshold level is set at the cost of lower sensitivity [98–101].

The use of multiple approaches resulted in a comprehensive computational method that predicted miRNA target interactions with the optimal or 'best' outcomes (Figures 2 and 5). Previous studies conducted to identify plant host-delivered miRNAs have also predicted the gene silencing targets in plant virus genomes with in silico tools. The successful experi-

mental in vivo evaluation of plant host genome-encoded miRNAs targeting different plant viruses has been reported [32,52,102]. The goal of this research was to apply computational approaches to predict the most optimal cotton miRNAs in the CLCuKoV-Lu genome to combat begomovirus infection of cotton transformed with miRNAs.

The application of RNAi to cotton varietal improvement to combat CLCuD infection offers a superior strategy for decreasing cotton yield loss [103–106]. However, gene pyramiding for enhanced resistance to CLCuKoV-Lu for upland cotton is complicated because of the allotetraploid nature of the cotton genome. The low regeneration efficiency of cotton callus is another constraint to the development of CLCuD-resistant (allotetraploid) upland cotton. The differential expression profile of ghr-miR2950 has been reported to combat early-stage infection of cotton by *V. dahlliae* infection [49,107,108]. The cotton miRNA, ghr-miR2950, exhibited differential expression in PHYA1 RNAi cotton [109]. The ghr-miR2950 is involved in gibberellin 3 hydroxylase expression [110], and it has been experimentally shown to accumulate at high levels in fibers while also being responsible for fiber cell elongation by GA signaling in *PHYA1* RNAi cotton plants [109,111]. Further, a ghr-miR2950 was identified and demonstrated to be involved in the growth and development of ovule and fiber in cotton, as well as in root-knot nematode (RKN) infection [112,113].

Finally, RNAi has been used for screening host plant-delivered factors for identifying various cellular functions against viruses [114–116]. In this study, a bioinformatics workflow has been developed that is expected to achieve CLCuKoV-Lu genome silencing as an antiviral capacity. Here, the design, construction, and in silico validation of an optimal amiRNA is reported, which is expected to result in the formation of a modified miRNA/miRNA* duplex via the precursor ghr-MIR-2950 (Figure 8). The results also add to the knowledge base required for minimizing the antiviral effects of cotton genome-encoded miRNAs to combat infection of CLCuKoV-Lu and related strains and potentially other CLCuD members of the complex.

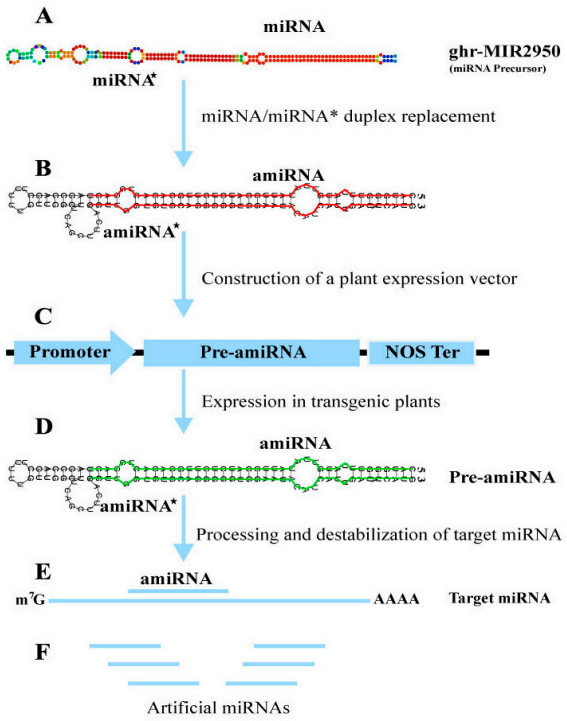

Figure 8. Mechanism of miRNA–mRNA gene silencing exploited for the development of CLCuKoV-resistant cotton. (**A**) Representative candidate consensus cotton precursor miRNA (ghr-MIR2950). (**B**) miRNA/miRNA duplex replacement. (**C**) Representative miRNA expression construct harboring the precursor sequenced driven by a promoter at the 5′ end and NOS terminator. (**D**) Mature amiRNA/amiRNA*duplex. (**E**) RISC processing of amiRNA. (**F**) Degradation of mRNA mediated by amiRNA.

5. Conclusions

CLCuKoV-Lu is a damaging pathogen of cotton and a predominant begomovirus species associated with the CLCuD epidemic in Pakistan. Infection by the virus results in reduced yield and quality in most cotton varieties cultivated in Pakistan. This research reports the application of optimized prediction tools and parameters for the identification of 'best-candidate miRNAs' predicted to show efficacy against CLCuKoV-Lu begomovirus infection of cotton.

To prepare for molecular cloning of effective miRNAs, in silico tools and approaches were evaluated and implemented to facilitate the predicted optimal binding affinity of mature candidate cotton miRNAs in the CLCuKoV-Lu genome. Among the 80 cotton miRNAs investigated, 4 consensus cotton locus-derived ghr-miRNAs were identified that are expected to base pair via miRNA–mRNA hybridization with miRNAs encoded by allotetraploid upland cotton and strains of CLCuKoV. The ghr-miR2950 was identified from among 80 miRNAs identified in cotton as the miRNA that shared the highest affinity for a conserved region of the CLCuKoV-Lu genome. Based on genome sequence comparisons of different CLCuKoV strains, the microRNA-binding region is conserved among CLCuKoV genomes, suggesting the likelihood of achieving species-wide protection with a single miRNA. Hence, mapping cotton miRNA–mRNA target interactions can result in untangling molecular underpinnings of cotton genetics in relation to its co-evolution with CLCuD-associated begomovirus pathogens.

Supplementary Materials: The following supporting information can be downloaded at: https://www.mdpi.com/article/10.3390/microbiolres15010001/s1, Table S1: List of mature *G. hirsutum* ghr-miRNA; Table S2: List of *G. hirsutum* precursor miRNAs; Table S3: Identification of binding sites of ghr-miRNAs in the CLCuKoV-Lu genome; Table S4: Gene-wise analysis of predicted miRNA and File S1: Prediction results analyzed by computational algorithms.

Author Contributions: M.A.A., J.K.B., M.S.I. and N.Y. conceived of the concept, approaches, and data interpretation. M.A.A. carried out the experiments and carried out the initial data analysis. All of the authors participated in the analysis and interpretation of the in silico data and in the editing of the draft manuscript. M.A.A. wrote the first draft of the manuscript. All authors have read and agreed to the published version of the manuscript.

Funding: This research was funded by the Central Public-interest Scientific Institution Basal Research Fund (1630052023003), Hainan Provincial Natural Science Foundation (322RC769), the open project of Guangxi Key Laboratory of Biology for Mango (GKLBM02203). The research work was completed under a MoU among the participating academic institutions.

Institutional Review Board Statement: Not applicable.

Informed Consent Statement: Not applicable.

Acknowledgments: The authors acknowledge the IPFP of HEC and TYSP of China to support M.A.A. The research was conducted through a collaboration outlined in an MoU between Khwaja Fareed University of Engineering and Information Technology and the Chinese Academy of Tropical Agricultural Sciences, as well as collaboration with The University of Arizona.

Conflicts of Interest: The authors declare they have no conflicts of interest.

References

1. Li, S.; Geng, S.; Pang, B.; Zhao, J.; Huang, Y.; Rui, C.; Cui, J.; Jiao, Y.; Zhang, R.; Gao, W. Revealing Genetic Differences in Fiber Elongation between the Offspring of Sea Island Cotton and Upland Cotton Backcross Populations Based on Transcriptome and Weighted Gene Coexpression Networks. *Genes* **2022**, *13*, 954. [CrossRef] [PubMed]
2. Jan, M.; Liu, Z.; Guo, C.; Sun, X. Molecular Regulation of Cotton Fiber Development: A Review. *Int. J. Mol. Sci.* **2022**, *23*, 5004. [CrossRef] [PubMed]
3. Townsend, T. World natural fibre production and employment. In *Handbook of Natural Fibres*; Elsevier: Amsterdam, The Netherlands, 2020; pp. 15–36.
4. Beasley, J. The origin of American tetraploid Gossypium species. *Am. Nat.* **1940**, *74*, 285–286. [CrossRef]

5. Skovsted, A. Cytological studies in cotton: IV. Chromosome conjugation in interspecific hybrids. *J. Genet.* **1937**, *34*, 97–134. [CrossRef]
6. Zhang, T.; Hu, Y.; Jiang, W.; Fang, L.; Guan, X.; Chen, J.; Zhang, J.; Saski, C.A.; Scheffler, B.E.; Stelly, D.M. Sequencing of allotetraploid cotton (*Gossypium hirsutum* L. acc. TM-1) provides a resource for fiber improvement. *Nat. Biotechnol.* **2015**, *33*, 531–537. [CrossRef] [PubMed]
7. Briddon, R.W. Cotton leaf curl disease, a multicomponent begomovirus complex. *Mol. Plant Pathol.* **2003**, *4*, 427–434. [CrossRef] [PubMed]
8. Rahman, M.-u.; Khan, A.Q.; Rahmat, Z.; Iqbal, M.A.; Zafar, Y. Genetics and genomics of cotton leaf curl disease, its viral causal agents and whitefly vector: A way forward to sustain cotton fiber security. *Front. Plant Sci.* **2017**, *8*, 1157. [CrossRef]
9. Zubair, M.; Zaidi, S.S.-e.-A.; Shakir, S.; Farooq, M.; Amin, I.; Scheffler, J.A.; Scheffler, B.E.; Mansoor, S. Multiple begomoviruses found associated with cotton leaf curl disease in Pakistan in early 1990 are back in cultivated cotton. *Sci. Rep.* **2017**, *7*, 680. [CrossRef]
10. Biswas, K.K.; Bhattacharyya, U.K.; Palchoudhury, S.; Balram, N.; Kumar, A.; Arora, R.; Sain, S.K.; Kumar, P.; Khetarpal, R.K.; Sanyal, A. Dominance of recombinant cotton leaf curl Multan-Rajasthan virus associated with cotton leaf curl disease outbreak in northwest India. *PLoS ONE* **2020**, *15*, e0231886. [CrossRef]
11. Amrao, L.; Amin, I.; Shahid, M.S.; Briddon, R.W.; Mansoor, S. Cotton leaf curl disease in resistant cotton is associated with a single begomovirus that lacks an intact transcriptional activator protein. *Virus Res.* **2010**, *152*, 153–163. [CrossRef]
12. Ashraf, M.A.; Shahid, A.A.; Mohamed, B.B.; Dahab, A.A.; Bajwa, K.S.; Rao, A.Q.; Khan, M.A.U.; Ilyas, M.; Haider, M.S.; Husnain, T. Molecular characterization and phylogenetic analysis of a variant of highly infectious cotton leaf curl Burewala virus associated with CLCuD from Pakistan. *Aust. J. Crop Sci.* **2013**, *7*, 1113–1122.
13. Shuja, M.N.; Briddon, R.W.; Tahir, M. Identification of a distinct strain of cotton leaf curl Burewala virus. *Arch. Virol.* **2014**, *159*, 2787–2790. [CrossRef]
14. Chen, T.; Tang, Y.; Zhao, R.; He, Z. Identification of the cryptic species of *Bemisia tabaci* transmitting Cotton leaf curl Multan virus. *Acta Phytophylacica Sin.* **2016**, *43*, 91–98.
15. Nigam, D. Genomic variation and diversification in begomovirus genome in implication to host and vector adaptation. *Plants* **2021**, *10*, 1706. [CrossRef] [PubMed]
16. Chen, T.; Saeed, Q.; He, Z.; Lu, L. Transmission efficiency of Cotton leaf curl Multan virus by three cryptic species of *Bemisia tabaci* complex in cotton cultivars. *PeerJ* **2019**, *7*, e7788. [CrossRef] [PubMed]
17. Paredes-Montero, J.R.; Hameed, U.; Zia-Ur-Rehman, M.; Rasool, G.; Haider, M.S.; Herrmann, H.-W.; Brown, J.K. Demographic expansion of the predominant *Bemisia tabaci* (Gennadius) (Hemiptera: Aleyrodidae) mitotypes associated with the Cotton leaf curl virus epidemic in Pakistan. *Ann. Entomol. Soc. Am.* **2019**, *112*, 265–280. [CrossRef]
18. de Moya, R.S.; Brown, J.K.; Sweet, A.D.; Walden, K.K.; Paredes-Montero, J.R.; Waterhouse, R.M.; Johnson, K.P. Nuclear orthologs derived from whole genome sequencing indicate cryptic diversity in the *Bemisia tabaci* (Insecta: Aleyrodidae) complex of whiteflies. *Diversity* **2019**, *11*, 151. [CrossRef]
19. Brown, J.K.; Zerbini, F.M.; Navas-Castillo, J.; Moriones, E.; Ramos-Sobrinho, R.; Silva, J.C.; Fiallo-Olivé, E.; Briddon, R.W.; Hernández-Zepeda, C.; Idris, A. Revision of *Begomovirus* taxonomy based on pairwise sequence comparisons. *Arch. Virol.* **2015**, *160*, 1593–1619. [CrossRef]
20. Kumar, J.; Kumar, A.; Roy, J.; Tuli, R.; Khan, J. Identification and molecular characterization of begomovirus and associated satellite DNA molecules infecting *Cyamopsis tetragonoloba*. *Virus Genes* **2010**, *41*, 118–125. [CrossRef]
21. Ashraf, M.A.; Shahid, A.A.; Rao, A.Q.; Bajwa, K.S.; Husnain, T. Functional characterization of a bidirectional plant promoter from cotton leaf curl Burewala virus using an *Agrobacterium*-mediated transient assay. *Viruses* **2014**, *6*, 223–242. [CrossRef]
22. Ashraf, M.A.; Shahid, A.A.; Rao, A.Q.; Brown, J.K.; Husnain, T. Development and Evaluation of the Cotton Leaf Curl Kokhran Virus-Burewala Bidirectional Promoter for Enhanced Cry1Ac Endotoxin Expression in Bt Transgenic Cotton. *Appl. Sci.* **2022**, *12*, 11275. [CrossRef]
23. Bornancini, V.A.; Irazoqui, J.M.; Flores, C.R.; Vaghi Medina, C.G.; Amadio, A.F.; López Lambertini, P.M. Reconstruction and characterization of full-length begomovirus and alphasatellite genomes infecting pepper through metagenomics. *Viruses* **2020**, *12*, 202. [CrossRef]
24. Palchoudhury, S.; Khare, V.; Balram, N.; Bhattacharyya, U.; Das, S.; Shukla, P.; Chakraborty, P.; Biswas, K. A multiplex polymerase chain reaction for the simultaneous detection of the virus and satellite components associated with cotton leaf curl begomovirus disease complex. *J. Virol. Methods* **2022**, *300*, 114369. [CrossRef] [PubMed]
25. Gawande, S.; Raghavendra, K.; Monga, D.; Nagrale, D.; Prabhulinga, T.; Hiremani, N.; Meshram, M.; Kranthi, S.; Gokte-Narkhedkar, N.; Waghmare, V. Development of Loop Mediated Isothermal Amplification (LAMP): A new tool for rapid diagnosis of cotton leaf curl viral disease. *J. Virol. Methods* **2022**, *306*, 114541. [CrossRef] [PubMed]
26. Inoue-Nagata, A.K.; Albuquerque, L.C.; Rocha, W.B.; Nagata, T. A simple method for cloning the complete begomovirus genome using the bacteriophage φ29 DNA polymerase. *J. Virol. Methods* **2004**, *116*, 209–211. [CrossRef] [PubMed]
27. Shafiq, M.; Iqbal, Z.; Ali, I.; Abbas, Q.; Mansoor, S.; Briddon, R.W.; Amin, I. Real-time quantitative PCR assay for the quantification of virus and satellites causing leaf curl disease in cotton in Pakistan. *J. Virol. Methods* **2017**, *248*, 54–60. [CrossRef] [PubMed]
28. Haible, D.; Kober, S.; Jeske, H. Rolling circle amplification revolutionizes diagnosis and genomics of geminiviruses. *J. Virol. Methods* **2006**, *135*, 9–16. [CrossRef]

29. Ahmed, N.; Amin, I.; Zaidi, S.S.-e.-A.; Rahman, S.U.; Farooq, M.; Fauquet, C.M.; Mansoor, S. Circular DNA enrichment sequencing reveals the viral/satellites genetic diversity associated with the third epidemic of cotton leaf curl disease. *Biol. Methods Protoc.* **2021**, *6*, bpab005. [CrossRef]
30. Pan, L.-L.; Cui, X.-Y.; Chen, Q.-F.; Wang, X.-W.; Liu, S.-S. Cotton leaf curl disease: Which whitefly is the vector? *Phytopathology* **2018**, *108*, 1172–1183. [CrossRef]
31. Deng, Z.; Ma, L.; Zhang, P.; Zhu, H. Small RNAs Participate in Plant–Virus Interaction and Their Application in Plant Viral Defense. *Int. J. Mol. Sci.* **2022**, *23*, 696. [CrossRef]
32. Zhou, L.; Yuan, Q.; Ai, X.; Chen, J.; Lu, Y.; Yan, F. Transgenic Rice Plants Expressing Artificial miRNA Targeting the Rice Stripe Virus MP Gene Are Highly Resistant to the Virus. *Biology* **2022**, *11*, 332. [CrossRef] [PubMed]
33. Villegas-Estrada, B.; Sánchez, M.A.; Valencia-Jiménez, A. Foliar Infiltration of Virus-Derived Small Hairpin RNAs Triggers the RNAi Mechanism against the Cucumber Mosaic Virus. *Int. J. Mol. Sci.* **2022**, *23*, 4938. [CrossRef]
34. Akbar, S.; Wei, Y.; Zhang, M.-Q. RNA Interference: Promising Approach to Combat Plant Viruses. *Int. J. Mol. Sci.* **2022**, *23*, 5312. [CrossRef] [PubMed]
35. Kim, Y.J.; Zheng, B.; Yu, Y.; Won, S.Y.; Mo, B.; Chen, X. The role of Mediator in small and long noncoding RNA production in *Arabidopsis thaliana*. *EMBO J.* **2011**, *30*, 814–822. [CrossRef] [PubMed]
36. Fang, X.; Cui, Y.; Li, Y.; Qi, Y. Transcription and processing of primary microRNAs are coupled by Elongator complex in *Arabidopsis*. *Nat. Plants* **2015**, *1*, 15075. [CrossRef] [PubMed]
37. Manavella, P.A.; Koenig, D.; Weigel, D. Plant secondary siRNA production determined by microRNA-duplex structure. *Proc. Natl. Acad. Sci. USA* **2012**, *109*, 2461–2466. [CrossRef]
38. Hu, B.; Zhong, L.; Weng, Y.; Peng, L.; Huang, Y.; Zhao, Y.; Liang, X.-J. Therapeutic siRNA: State of the art. *Signal Transduct. Target. Ther.* **2020**, *5*, 101. [CrossRef]
39. Hung, Y.-H.; Slotkin, R.K. The initiation of RNA interference (RNAi) in plants. *Curr. Opin. Plant Biol.* **2021**, *61*, 102014. [CrossRef]
40. Reinhart, B.J.; Weinstein, E.G.; Rhoades, M.W.; Bartel, B.; Bartel, D.P. MicroRNAs in plants. *Genes Dev.* **2002**, *16*, 1616–1626. [CrossRef]
41. Cui, J.; You, C.; Chen, X. The evolution of microRNAs in plants. *Curr. Opin. Plant Biol.* **2017**, *35*, 61–67. [CrossRef]
42. Carrington, J.C.; Ambros, V. Role of microRNAs in plant and animal development. *Science* **2003**, *301*, 336–338. [CrossRef] [PubMed]
43. Wang, M.; Sun, R.; Li, C.; Wang, Q.; Zhang, B. MicroRNA expression profiles during cotton (*Gossypium hirsutum* L) fiber early development. *Sci. Rep.* **2017**, *7*, 44454. [CrossRef] [PubMed]
44. Zhao, T.; Xu, X.; Wang, M.; Li, C.; Li, C.; Zhao, R.; Zhu, S.; He, Q.; Chen, J. Identification and profiling of upland cotton microRNAs at fiber initiation stage under exogenous IAA application. *BMC Genom.* **2019**, *20*, 421. [CrossRef] [PubMed]
45. Zhang, J.; Ma, M.; Liu, Y.; Ismayil, A. Plant Defense and Viral Counter-Defense during Plant–Geminivirus Interactions. *Viruses* **2023**, *15*, 510. [CrossRef] [PubMed]
46. Li, J.; Hull, J.J.; Liang, S.; Wang, Q.; Chen, L.; Zhang, Q.; Wang, M.; Mansoor, S.; Zhang, X.; Jin, S. Genome-wide analysis of cotton miRNAs during whitefly infestation offers new insights into plant-herbivore interaction. *Int. J. Mol. Sci.* **2019**, *20*, 5357. [CrossRef] [PubMed]
47. Zhang, T.; Zhao, Y.-L.; Zhao, J.-H.; Wang, S.; Jin, Y.; Chen, Z.-Q.; Fang, Y.-Y.; Hua, C.-L.; Ding, S.-W.; Guo, H.-S. Cotton plants export microRNAs to inhibit virulence gene expression in a fungal pathogen. *Nat. Plants* **2016**, *2*, 16153. [CrossRef] [PubMed]
48. Wang, W.; Liu, D.; Chen, D.; Cheng, Y.; Zhang, X.; Song, L.; Hu, M.; Dong, J.; Shen, F. MicroRNA414c affects salt tolerance of cotton by regulating reactive oxygen species metabolism under salinity stress. *RNA Biol.* **2019**, *16*, 362–375. [CrossRef]
49. He, X.; Sun, Q.; Jiang, H.; Zhu, X.; Mo, J.; Long, L.; Xiang, L.; Xie, Y.; Shi, Y.; Yuan, Y. Identification of novel microRNAs in the Verticillium wilt-resistant upland cotton variety KV-1 by high-throughput sequencing. *SpringerPlus* **2014**, *3*, 564. [CrossRef]
50. Dong, Z.; Zhang, J.; Zhu, Q.; Zhao, L.; Sui, S.; Li, Z.; Zhang, Y.; Wang, H.; Tian, D.; Zhao, Y. Identification of microRNAs involved in drought stress responses in early-maturing cotton by high-throughput sequencing. *Genes Genom.* **2018**, *40*, 305–314. [CrossRef]
51. Zhang, H.; Feng, H.; Lu, X.; Wang, C.; Yang, W.; Li, F. An asymmetric bulge enhances artificial microRNA-mediated virus resistance. *Plant Biotechnol. J.* **2020**, *18*, 608. [CrossRef]
52. Niu, Q.-W.; Lin, S.-S.; Reyes, J.L.; Chen, K.-C.; Wu, H.-W.; Yeh, S.-D.; Chua, N.-H. Expression of artificial microRNAs in transgenic *Arabidopsis thaliana* confers virus resistance. *Nat. Biotechnol.* **2006**, *24*, 1420–1428. [CrossRef] [PubMed]
53. Kozomara, A.; Birgaoanu, M.; Griffiths-Jones, S. miRBase: From microRNA sequences to function. *Nucleic Acids Res.* **2019**, *47*, D155–D162. [CrossRef] [PubMed]
54. Sayers, E.W.; Beck, J.; Bolton, E.E.; Bourexis, D.; Brister, J.R.; Canese, K.; Comeau, D.C.; Funk, K.; Kim, S.; Klimke, W. Database resources of the national center for biotechnology information. *Nucleic Acids Res.* **2021**, *49*, D10. [CrossRef] [PubMed]
55. Enright, A.; John, B.; Gaul, U.; Tuschl, T.; Sander, C.; Marks, D. MicroRNA targets in *Drosophila*. *Genome Biol.* **2003**, *4*, P8. [CrossRef]
56. John, B.; Enright, A.J.; Aravin, A.; Tuschl, T.; Sander, C.; Marks, D.S. Human microRNA targets. *PLoS Biol.* **2004**, *2*, e363. [CrossRef]
57. Miranda, K.C.; Huynh, T.; Tay, Y.; Ang, Y.-S.; Tam, W.-L.; Thomson, A.M.; Lim, B.; Rigoutsos, I. A pattern-based method for the identification of MicroRNA binding sites and their corresponding heteroduplexes. *Cell* **2006**, *126*, 1203–1217. [CrossRef] [PubMed]
58. Loher, P.; Rigoutsos, I. Interactive exploration of RNA22 microRNA target predictions. *Bioinformatics* **2012**, *28*, 3322–3323. [CrossRef]

59. Dai, X.; Zhao, P.X. psRNATarget: A plant small RNA target analysis server. *Nucleic Acids Res.* **2011**, *39*, W155–W159. [CrossRef]
60. Dai, X.; Zhuang, Z.; Zhao, P.X. psRNATarget: A plant small RNA target analysis server (2017 release). *Nucleic Acids Res.* **2018**, *46*, W49–W54. [CrossRef]
61. Krüger, J.; Rehmsmeier, M. RNAhybrid: microRNA target prediction easy, fast and flexible. *Nucleic Acids Res.* **2006**, *34*, W451–W454. [CrossRef]
62. Lorenz, R.; Bernhart, S.H.; Höner zu Siederdissen, C.; Tafer, H.; Flamm, C.; Stadler, P.F.; Hofacker, I.L. ViennaRNA Package 2.0. *Algorithms Mol. Biol.* **2011**, *6*, 26. [CrossRef] [PubMed]
63. Bernhart, S.H.; Tafer, H.; Mückstein, U.; Flamm, C.; Stadler, P.F.; Hofacker, I.L. Partition function and base pairing probabilities of RNA heterodimers. *Algorithms Mol. Biol.* **2006**, *1*, 3. [CrossRef] [PubMed]
64. Krzywinski, M.; Schein, J.; Birol, I.; Connors, J.; Gascoyne, R.; Horsman, D.; Jones, S.J.; Marra, M.A. Circos: An information aesthetic for comparative genomics. *Genome Res.* **2009**, *19*, 1639–1645. [CrossRef]
65. Kumar, S.; Stecher, G.; Li, M.; Knyaz, C.; Tamura, K. MEGA X: Molecular evolutionary genetics analysis across computing platform. *Mol. Biol. Evol.* **2018**, *35*, 1547–1549. [CrossRef] [PubMed]
66. Edgar, R.C. MUSCLE: A multiple sequence alignment method with reduced time and space complexity. *BMC Bioinform.* **2004**, *5*, 1–19. [CrossRef] [PubMed]
67. Błażewicz, J.; Formanowicz, P.; Kasprzak, M.; Michalak, K.; Wierzejewski, P. Clustal W algorithm for multiple sequence alignment revisited. *Found. Comput. Decis. Sci.* **2001**, *26*, 189–196.
68. Gandrud, C. *Reproducible Research with R and RStudio*; Chapman and Hall/CRC: Boca Raton, FL, USA, 2018.
69. Fan, Y.-Y.; Zhong, Y.-W.; Zhao, J.; Chi, Y.; Bouvaine, S.; Liu, S.-S.; Seal, S.E.; Wang, X.-W. *Bemisia tabaci* vesicle-associated membrane protein 2 interacts with begomoviruses and plays a role in virus acquisition. *Cells* **2021**, *10*, 1700. [CrossRef] [PubMed]
70. Götz, M.; Popovski, S.; Kollenberg, M.; Gorovits, R.; Brown, J.K.; Cicero, J.M.; Czosnek, H.; Winter, S.; Ghanim, M. Implication of *Bemisia tabaci* heat shock protein 70 in begomovirus-whitefly interactions. *J. Virol.* **2012**, *86*, 13241–13252. [CrossRef]
71. Poornima Priyadarshini, C.; Ambika, M.; Tippeswamy, R.; Savithri, H. Functional characterization of coat protein and V2 involved in cell to cell movement of Cotton leaf curl Kokhran virus-Dabawali. *PLoS ONE* **2011**, *6*, e26929. [CrossRef]
72. Bahari, A.; Castillo, A.G.; Safaie, N.; Bejarano, E.R.; Luna, A.P.; Shams-Bakhsh, M. Functional analysis of V2 protein of Beet curly top Iran virus. *Plants* **2022**, *11*, 3351. [CrossRef]
73. Li, M.; Li, C.; Jiang, K.; Li, K.; Zhang, J.; Sun, M.; Wu, G.; Qing, L. Characterization of pathogenicity-associated V2 protein of tobacco curly shoot virus. *Int. J. Mol. Sci.* **2021**, *22*, 923. [CrossRef] [PubMed]
74. Wang, Y.; Wu, Y.; Gong, Q.; Ismayil, A.; Yuan, Y.; Lian, B.; Jia, Q.; Han, M.; Deng, H.; Hong, Y. Geminiviral V2 protein suppresses transcriptional gene silencing through interaction with AGO4. *J. Virol.* **2019**, *93*, e01675-18. [CrossRef] [PubMed]
75. Hipp, K.; Rau, P.; Schäfer, B.; Gronenborn, B.; Jeske, H. The RXL motif of the African cassava mosaic virus Rep protein is necessary for rereplication of yeast DNA and viral infection in plants. *Virology* **2014**, *462*, 189–198. [CrossRef] [PubMed]
76. Xu, X.; Zhang, Q.; Hong, J.; Li, Z.; Zhang, X.; Zhou, X. Cryo-EM structure of a begomovirus geminate particle. *Int. J. Mol. Sci.* **2019**, *20*, 1738. [CrossRef] [PubMed]
77. Torres-Herrera, S.I.; Romero-Osorio, A.; Moreno-Valenzuela, O.; Pastor-Palacios, G.; Cardenas-Conejo, Y.; Ramírez-Prado, J.H.; Riego-Ruiz, L.; Minero-García, Y.; Ambriz-Granados, S.; Argüello-Astorga, G.R. A lineage of begomoviruses encode Rep and AC4 proteins of enigmatic ancestry: Hints on the evolution of geminiviruses in the New World. *Viruses* **2019**, *11*, 644. [CrossRef] [PubMed]
78. Guerrero, J.; Regedanz, E.; Lu, L.; Ruan, J.; Bisaro, D.M.; Sunter, G. Manipulation of the plant host by the geminivirus AC2/C2 protein, a central player in the infection cycle. *Front. Plant Sci.* **2020**, *11*, 591. [CrossRef]
79. Rosas-Díaz, T.; Macho, A.P.; Beuzón, C.R.; Lozano-Durán, R.; Bejarano, E.R. The C2 protein from the geminivirus *Tomato yellow leaf curl Sardinia virus* decreases sensitivity to jasmonates and suppresses jasmonate-mediated defences. *Plants* **2016**, *5*, 8. [CrossRef]
80. Veluthambi, K.; Sunitha, S. Targets and mechanisms of geminivirus silencing suppressor protein AC2. *Front. Microbiol.* **2021**, *12*, 645419. [CrossRef]
81. Settlage, S.B.; See, R.G.; Hanley-Bowdoin, L. Geminivirus C3 protein: Replication enhancement and protein interactions. *J. Virol.* **2005**, *79*, 9885–9895. [CrossRef]
82. Fondong, V.N. Geminivirus protein structure and function. *Mol. Plant Pathol.* **2013**, *14*, 635–649. [CrossRef]
83. Medina-Puche, L.; Orílio, A.F.; Zerbini, F.M.; Lozano-Durán, R. Small but mighty: Functional landscape of the versatile geminivirus-encoded C4 protein. *PLoS Pathog.* **2021**, *17*, e1009915. [CrossRef]
84. Dai, K.-W.; Tsai, Y.-T.; Wu, C.-Y.; Lai, Y.-C.; Lin, N.-S.; Hu, C.-C. Identification of Crucial Amino Acids in *Begomovirus* C4 Proteins Involved in the Modulation of the Severity of Leaf Curling Symptoms. *Viruses* **2022**, *14*, 499. [CrossRef] [PubMed]
85. Khan, Z.A.; Abdin, M.Z.; Khan, J.A. Functional characterization of a strong bi-directional constitutive plant promoter isolated from cotton leaf curl Burewala virus. *PLoS ONE* **2015**, *10*, e0121656. [CrossRef]
86. Brodersen, P.; Sakvarelidze-Achard, L.; Bruun-Rasmussen, M.; Dunoyer, P.; Yamamoto, Y.Y.; Sieburth, L.; Voinnet, O. Widespread translational inhibition by plant miRNAs and siRNAs. *Science* **2008**, *320*, 1185–1190. [CrossRef] [PubMed]
87. Siddique, Z.; Akhtar, K.P.; Hameed, A.; Sarwar, N.; Imran-Ul-Haq; Khan, S.A. Biochemical alterations in leaves of resistant and susceptible cotton genotypes infected systemically by cotton leaf curl Burewala virus. *J. Plant Interact.* **2014**, *9*, 702–711. [CrossRef]
88. Amrao, L.; Akhter, S.; Tahir, M.N.; Amin, I.; Briddon, R.W.; Mansoor, S. Cotton leaf curl disease in Sindh province of Pakistan is associated with recombinant begomovirus components. *Virus Res.* **2010**, *153*, 161–165. [CrossRef] [PubMed]

89. Ashraf, M.A.; Tariq, H.K.; Hu, X.-W.; Khan, J.; Zou, Z. Computational Biology and Machine Learning Approaches Identify Rubber Tree (*Hevea brasiliensis* Muell. Arg.) Genome Encoded MicroRNAs Targeting Rubber Tree Virus 1. *Appl. Sci.* **2022**, *12*, 12908. [CrossRef]
90. Ashraf, M.A.; Feng, X.; Hu, X.; Ashraf, F.; Shen, L.; Iqbal, M.S.; Zhang, S. In silico identification of sugarcane (*Saccharum officinarum* L.) genome encoded microRNAs targeting sugarcane bacilliform virus. *PLoS ONE* **2022**, *17*, e0261807. [CrossRef]
91. Ashraf, M.A.; Ashraf, F.; Feng, X.; Hu, X.; Shen, L.; Khan, J.; Zhang, S. Potential targets for evaluation of sugarcane yellow leaf virus resistance in sugarcane cultivars: In silico sugarcane miRNA and target network prediction. *Biotechnol. Biotechnol. Equip.* **2021**, *35*, 1980–1991. [CrossRef]
92. Shahid, M.N.; Rasheed, S.; Iqbal, M.S.; Jamal, A.; Khalid, S.; Shamim, Z. In silico prediction of potential miRNAs to target zymv in *Cucumis melo*. *Pak. J. Bot* **2022**, *54*, 1319–1325.
93. Ashraf, F.; Ashraf, M.A.; Hu, X.; Zhang, S. A novel computational approach to the silencing of *Sugarcane Bacilliform Guadeloupe A Virus* determines potential host-derived MicroRNAs in sugarcane (*Saccharum officinarum* L.). *PeerJ* **2020**, *8*, e8359. [CrossRef] [PubMed]
94. Gaafar, Y.Z.A.; Ziebell, H. Novel targets for engineering Physostegia chlorotic mottle and tomato brown rugose fruit virus-resistant tomatoes: In silico prediction of tomato microRNA targets. *PeerJ* **2020**, *8*, e10096. [CrossRef]
95. Jabbar, B.; Iqbal, M.S.; Batcho, A.A.; Nasir, I.A.; Rashid, B.; Husnain, T.; Henry, R.J. Target prediction of candidate miRNAs from *Oryza sativa* for silencing the RYMV genome. *Comput. Biol. Chem.* **2019**, *83*, 107127. [CrossRef] [PubMed]
96. Iqbal, M.S.; Jabbar, B.; Sharif, M.N.; Ali, Q.; Husnain, T.; Nasir, I.A. In silico MCMV silencing concludes potential host-derived miRNAs in maize. *Front. Plant Sci.* **2017**, *8*, 372. [CrossRef] [PubMed]
97. Ashraf, M.A.; Ali, B.; Brown, J.K.; Shahid, I.; Yu, N. In Silico Identification of Cassava Genome-Encoded MicroRNAs with Predicted Potential for Targeting the ICMV-Kerala Begomoviral Pathogen of Cassava. *Viruses* **2023**, *15*, 486. [CrossRef]
98. Quillet, A.; Anouar, Y.; Lecroq, T.; Dubessy, C. Prediction methods for microRNA targets in bilaterian animals: Toward a better understanding by biologists. *Comput. Struct. Biotechnol. J.* **2021**, *19*, 5811–5825. [CrossRef] [PubMed]
99. Oliveira, A.C.; Bovolenta, L.A.; Nachtigall, P.G.; Herkenhoff, M.E.; Lemke, N.; Pinhal, D. Combining results from distinct microRNA target prediction tools enhances the performance of analyses. *Front. Genet.* **2017**, *8*, 59. [CrossRef]
100. Min, H.; Yoon, S. Got target?: Computational methods for microRNA target prediction and their extension. *Exp. Mol. Med.* **2010**, *42*, 233–244. [CrossRef]
101. Riffo-Campos, Á.L.; Riquelme, I.; Brebi-Mieville, P. Tools for sequence-based miRNA target prediction: What to choose? *Int. J. Mol. Sci.* **2016**, *17*, 1987. [CrossRef]
102. Petchthai, U.; Yee, C.S.L.; Wong, S.-M. Resistance to CymMV and ORSV in artificial microRNA transgenic *Nicotiana benthamiana* plants. *Sci. Rep.* **2018**, *8*, 9958. [CrossRef]
103. Akhtar, S.; Tahir, M.N.; Amin, I.; Mansoor, S. Amplicon-based RNAi construct targeting beta-C1 gene gives enhanced resistance against cotton leaf curl disease. *3 Biotech* **2021**, *11*, 256. [CrossRef] [PubMed]
104. Ahmad, A.; Zia-Ur-Rehman, M.; Hameed, U.; Qayyum Rao, A.; Ahad, A.; Yasmeen, A.; Akram, F.; Bajwa, K.S.; Scheffler, J.; Nasir, I.A. Engineered disease resistance in cotton using RNA-interference to knock down Cotton leaf curl Kokhran virus-Burewala and Cotton leaf curl Multan betasatellite expression. *Viruses* **2017**, *9*, 257. [CrossRef] [PubMed]
105. Yasmeen, A.; Kiani, S.; Butt, A.; Rao, A.Q.; Akram, F.; Ahmad, A.; Nasir, I.A.; Husnain, T.; Mansoor, S.; Amin, I. Amplicon-based RNA interference targeting V2 gene of *cotton leaf curl Kokhran Virus*-Burewala strain can provide resistance in transgenic cotton plants. *Mol. Biotechnol.* **2016**, *58*, 807–820. [CrossRef] [PubMed]
106. Ali, I.; Amin, I.; Briddon, R.W.; Mansoor, S. Artificial microRNA-mediated resistance against the monopartite begomovirus Cotton leaf curl Burewala virus. *Virol. J.* **2013**, *10*, 1–8. [CrossRef] [PubMed]
107. Yin, Z.; Li, Y.; Han, X.; Shen, F. Genome-wide profiling of miRNAs and other small non-coding RNAs in the *Verticillium dahliae*–inoculated cotton roots. *PLoS ONE* **2012**, *7*, e35765. [CrossRef] [PubMed]
108. Zhang, Y.; Wang, W.; Chen, J.; Liu, J.; Xia, M.; Shen, F. Identification of miRNAs and their targets in cotton inoculated with *Verticillium dahliae* by high-throughput sequencing and degradome analysis. *Int. J. Mol. Sci.* **2015**, *16*, 14749–14768. [CrossRef] [PubMed]
109. Miao, Q.; Deng, P.; Saha, S.; Jenkins, J.N.; Hsu, C.-Y.; Abdurakhmonov, I.Y.; Buriev, Z.T.; Pepper, A.; Ma, D.-P. Genome-wide identification and characterization of microRNAs differentially expressed in fibers in a cotton phytochrome A1 RNAi line. *PLoS ONE* **2017**, *12*, e0179381. [CrossRef]
110. Pang, M.; Woodward, A.W.; Agarwal, V.; Guan, X.; Ha, M.; Ramachandran, V.; Chen, X.; Triplett, B.A.; Stelly, D.M.; Chen, Z.J. Genome-wide analysis reveals rapid and dynamic changes in miRNA and siRNA sequence and expression during ovule and fiber development in allotetraploid cotton (*Gossypium hirsutum* L.). *Genome Biol.* **2009**, *10*, R122. [CrossRef]
111. Hedden, P.; Kamiya, Y. Gibberellin biosynthesis: Enzymes, genes and their regulation. *Annu. Rev. Plant Biol.* **1997**, *48*, 431–460. [CrossRef]
112. Cai, C.; Li, C.; Sun, R.; Zhang, B.; Nichols, R.L.; Hake, K.D.; Pan, X. Small RNA and degradome deep sequencing reveals important roles of microRNAs in cotton (*Gossypium hirsutum* L.) response to root-knot nematode *Meloidogyne incognita* infection. *Genomics* **2021**, *113*, 1146–1156. [CrossRef]
113. Pan, X.; Nichols, R.L.; Li, C.; Zhang, B. MicroRNA-target gene responses to root knot nematode (*Meloidogyne incognita*) infection in cotton (*Gossypium hirsutum* L.). *Genomics* **2019**, *111*, 383–390. [CrossRef] [PubMed]

114. Hirsch, A.J. The use of RNAi-based screens to identify host proteins involved in viral replication. *Future Microbiol.* **2010**, *5*, 303–311. [CrossRef] [PubMed]
115. Kampmann, M.; Horlbeck, M.A.; Chen, Y.; Tsai, J.C.; Bassik, M.C.; Gilbert, L.A.; Villalta, J.E.; Kwon, S.C.; Chang, H.; Kim, V.N. Next-generation libraries for robust RNA interference-based genome-wide screens. *Proc. Natl. Acad. Sci. USA* **2015**, *112*, E3384–E3391. [CrossRef] [PubMed]
116. Martin, S.; Chiramel, A.I.; Schmidt, M.L.; Chen, Y.-C.; Whitt, N.; Watt, A.; Dunham, E.C.; Shifflett, K.; Traeger, S.; Leske, A. A genome-wide siRNA screen identifies a druggable host pathway essential for the Ebola virus life cycle. *Genome Med.* **2018**, *10*, 58. [CrossRef]